

## THE ORIGIN OF THE HEAVIEST METALS IN MOST ULTRA-FAINT DWARF GALAXIES

IAN U. ROEDERER<sup>1,2</sup>

*Accepted for publication in the Astrophysical Journal*

### ABSTRACT

The heaviest metals found in stars in most ultra-faint dwarf (UFD) galaxies in the Milky Way halo are generally underabundant by an order of magnitude or more when compared with stars in the halo field. Among the heavy elements produced by  $n$ -capture reactions, only Sr and Ba can be detected in red giant stars in most UFD galaxies. This limited chemical information is unable to identify the nucleosynthesis process(es) responsible for producing the heavy elements in UFD galaxies. Similar [Sr/Ba] and [Ba/Fe] ratios are found in three bright halo field stars, BD-18°5550, CS 22185-007, and CS 22891-200. Previous studies of high-quality spectra of these stars report detections of additional  $n$ -capture elements, including Eu. The [Eu/Ba] ratios in these stars span +0.41 to +0.86. These ratios and others among elements in the rare earth domain indicate an  $r$ -process origin. These stars have some of the lowest levels of  $r$ -process enhancement known, with [Eu/H] spanning -3.95 to -3.32, and they may be considered nearby proxies for faint stars in UFD galaxies. Direct confirmation, however, must await future observations of additional heavy elements in stars in the UFD galaxies themselves.

*Subject headings:* galaxies: dwarf — Galaxy: halo — nuclear reactions, nucleosynthesis, abundances — stars: abundances

### 1. INTRODUCTION

Stars found in the lowest luminosity galaxies known reveal the chemical composition of the molecular clouds seeded by metals produced by only one or a few prior generations of stars. These ultra-faint dwarf (UFD) galaxies date from the early Universe (e.g., Brown et al. 2014). The elements found within their stars inform our understanding of the first stars, the first metal production, the process of galaxy formation, and the nature of the building blocks of our own Milky Way.

High-resolution optical spectra have been obtained and analyzed for individual stars in 11 UFD galaxies around the Milky Way. These galaxies range from 23 to 160 kpc from the Sun (McConnachie 2012; Bechtol et al. 2015), and the faintness of their brightest red giant stars (typically  $16 < V < 19$ ) limits the quantity and quality of high-resolution spectra that can be obtained. Even so, elements heavier than the iron group—Sr ( $Z = 38$ ) or Ba ( $Z = 56$ )—have been detected in all but one (Boo II; François et al. 2016; Ji et al. 2016d) of these galaxies and nearly all halo field stars that have been studied (Roederer 2013). As detailed chemical abundances have been presented for stars in more UFD galaxies, a consistent, if yet unexplained, pattern has emerged. In general, the heaviest elements are underabundant relative to Fe or H when compared with halo field stars at similar metallicities (e.g., Koch et al. 2013; Frebel & Norris 2015).

Other heavy elements are rarely detected in stars in the UFD galaxies. These elements could be present yet remain undetectable because their abundances are even lower than Sr and Ba and their electronic transitions are not concentrated in a few strong lines in the same way that Sr II and Ba II are (e.g., Roederer 2013). Frebel et al. (2010) made the first detection of La ( $Z = 57$ ) in any

UFD, and Frebel et al. (2014) made the first detections of elements heavier than La in any UFD. These detections were possible because the stars in question probably were enriched after their birth by  $s$ -process material from a more evolved binary companion star that passed through the asymptotic giant branch (AGB) phase of evolution.

It was not until the detection of high levels of  $r$ -process enhancement in many stars in Ret II that elements heavier than Ba were detected in any UFD star whose present-day composition reflects its natal composition (Ji et al. 2016a,c; Roederer et al. 2016b). In the case of Ret II, the nucleosynthesis process responsible for the production of the heavy elements in these stars is easily identified as the  $r$ -process because so many elements are detectable. Ji et al. (2016a) conclude that any rare site that produces a large yield of  $r$ -process material is consistent with the constraints imposed by Ret II. Lee et al. (2013) anticipated this outcome, and their chemical evolution models assumed a strong mass-dependent yield of  $r$ -process material from a small fraction of core-collapse supernovae. Even if the astrophysical site associated with the  $r$ -process material in Ret II cannot be unambiguously identified, identifying an environment teeming with  $r$ -process material is an important step toward this goal.

Setting Ret II aside, the stars in UFD galaxies with low levels of  $n$ -capture elements are distinct in their [Sr/Ba] and [Ba/Fe] ratios relative to the majority of halo field stars (Ji et al. 2016c). Frebel & Norris (2015) surmised that these low, distinct heavy-element abundances could be a signature of the earliest star-forming clouds. If so, this raises the tantalizing possibility of identifying the first  $n$ -capture process to have operated in the early Universe, perhaps even in the first stars.

What was that process? At present, the answer is unclear. Other work on candidate second-generation stars in the halo field implicates some form of  $r$ -process nucleosynthesis (Roederer et al. 2014b). Only one ratio—

<sup>1</sup> Department of Astronomy, University of Michigan, 1085 S. University Ave., Ann Arbor, MI 48109, USA; iur@umich.edu

<sup>2</sup> Joint Institute for Nuclear Astrophysics and Center for the Evolution of the Elements (JINA-CEE), USA

[Sr/Ba]—is available in the stars in UFD galaxies, so it is difficult to exclude candidate processes. In principle, it should be possible to detect additional heavy elements in the spectra of individual metal-poor red giant stars in the UFD galaxies with higher signal-to-noise (S/N) spectra. In practice, obtaining such spectra is extremely challenging because large-aperture telescope time is limited and these stars are so faint. A more tractable approach could be to examine nearby, bright halo field stars. Additional  $n$ -capture elements may be detectable in the high S/N spectra of the few bright halo field stars that occupy the same region of chemical space as the stars in most UFD galaxies. Here, I identify three such stars with low levels of  $n$ -capture elements. The chemical composition of these halo field stars is likely to be similar to the stars in most UFD galaxies. These stars may represent our best opportunity to identify the nucleosynthesis process(es) responsible for producing the  $n$ -capture elements found in extremely low levels in the UFD galaxies.

## 2. LITERATURE SAMPLE

Figure 1 illustrates the [Sr/Ba] and [Ba/Fe] ratios for 977 metal-poor ( $[\text{Fe}/\text{H}] < -1.5$ ) stars in the halo field (951 stars) and UFD galaxies (26 stars). The literature sources are listed in Table 1. Duplicates have been removed from the sample. The abundance data for the field stars are taken mainly from recent large surveys, supplemented with data from studies of individual stars. Consequently, this is not an unbiased sample. Nevertheless, it is useful for the purpose of the present study simply because it populates the region of interest in Figure 1.

The shaded region in Figure 1 highlights the parameter space where most stars in UFD galaxies are found. This region spans several dex in [Sr/Ba], and it is offset to lower [Ba/Fe] by more than 1 dex from the main locus of halo field stars. Each of the 85 halo field stars found in this region is a candidate for further consideration. I require that both Sr and Ba be detected in a given star. This is a practical choice, because stars with no detectable Sr or Ba are unlikely to have detections from weaker lines of less abundant elements.

Most of the stars (seven of nine) that have been studied in the Ret II UFD galaxy are highly enhanced in  $r$ -process material, unlike the remaining two stars in Ret II and stars in the other 10 UFD galaxies that have been studied. The seven  $r$ -process-enhanced stars in Ret II are circled with the bold line in Figure 1.

Detailed abundances have been studied in three other UFD galaxies that are not illustrated in Figure 1, Boo II, CVn II, and Seg 1. Sr and Ba have been detected in Seg 1, but not simultaneously in any given star with  $[\text{Fe}/\text{H}] < -1.5$  (Frebel et al. 2014). One star has been studied in CVn II, and only Sr has been detected there (François et al. 2016). At present, only Boo II lacks any compelling detection of Sr or Ba, though only four stars in Boo II have been examined (Koch & Rich 2014; François et al. 2016; Ji et al. 2016d). Upper limits on Sr and Ba in stars in Boo II, CVn II, and Seg 1 suggest they occupy similar regions of parameter space as the stars in other UFD galaxies (e.g., Frebel et al. 2014; Ji et al. 2016c).

## 3. RESULTS

**Table 1**  
Literature Sources for Abundance Data

Reference	No. stars	Population
Aoki et al. (2002)	2	field
Aoki et al. (2004)	1	field
Aoki et al. (2005)	14	field
Aoki et al. (2006)	1	field
Aoki et al. (2010)	2	field
Aoki et al. (2013a)	35	field
Barklem et al. (2005)	200	field
Bonifacio et al. (2009)	5	field
Burris et al. (2000)	9	field
Carretta et al. (2002)	5	field
Cohen et al. (2008)	1	field
Cohen et al. (2013)	80	field
Depagne et al. (2000)	1	field
François et al. (2007)	30	field
François et al. (2016)	2	Her
Frebel et al. (2010)	6	Com, UMa II
Frebel et al. (2016)	2	Boo I
Gratton & Sneden (1994)	2	field
Hansen et al. (2011)	1	field
Hansen et al. (2015)	15	field
Hollek et al. (2011)	16	field
Honda et al. (2004)	8	field
Honda et al. (2011)	1	field
Ishigaki et al. (2014)	2	Boo I
Ivans et al. (2003)	1	field
Jacobson et al. (2015)	115	field
Ji et al. (2016c)	7	Ret II
Ji et al. (2016b)	4	Tuc II
Johnson (2002)	13	field
Lai et al. (2007)	53	field
Lai et al. (2008)	21	field
Mashonkina et al. (2010)	1	field
Mashonkina et al. (2014)	1	field
McWilliam (1998)	3	field
Mishenina & Kovtyukh (2001)	6	field
Norris et al. (2010)	1	Boo I
Placco et al. (2015)	1	field
Placco et al. (2016)	1	field
Preston & Sneden (2000)	14	field
Preston & Sneden (2001)	2	field
Preston et al. (2006)	6	field
Roederer et al. (2010)	1	field
Roederer & Kirby (2014)	1	Seg 2
Roederer et al. (2014c)	259	field
Roederer et al. (2016a)	1	field
Roederer & Lawler (2012)	1	field
Ryan et al. (1991)	3	field
Ryan et al. (1996)	2	field
Simon et al. (2010)	1	Leo IV
Sivarani et al. (2006)	2	field
Sneden et al. (2003b)	2	field
Yong et al. (2013)	13	field

Most halo field stars in the shaded region of Figure 1 lack any additional detections of heavy elements other than Sr and Ba, as might be expected given the low abundances. A few stars show detections of Y ( $Z = 39$ ) or Zr ( $Z = 40$ ), but these elements offer little new information that could be used to distinguish the nucleosynthesis mechanism responsible for producing the heavy elements. Only three stars show compelling detections of one or more elements heavier than Ba: BD-18°5550, CS 22185-007, and CS 22891-200. Their heavy element abundance patterns are illustrated in Figure 2. The fact that these three stars lie near the right side of the shaded region is not surprising, because detection becomes increasingly difficult as the overall abundances decrease from right to left.

BD-18°5550 is a bright ( $V \approx 9.3$ ) metal-poor

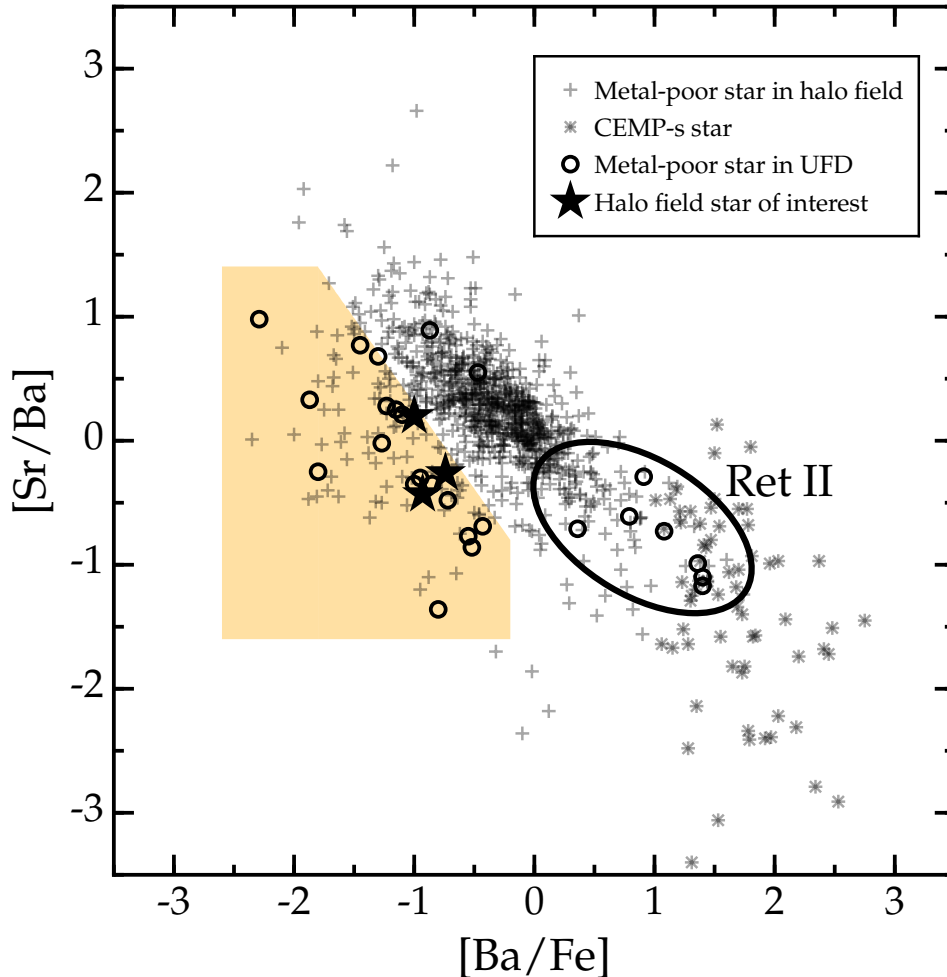


**Figure 1.** Sr and Ba abundances in field stars and stars in UFD galaxies. The crosses mark individual metal-poor ( $[\text{Fe}/\text{H}] < -1.5$ ) stars in the halo field, the circles mark individual metal-poor stars in UFD galaxies, and the large star-shaped symbols mark the three field stars of interest: BD-18°5550, CS 22185-007, and CS 22891-200. Halo stars marked with an eight-pointed shape are suspected to have received large amounts of carbon and  $s$ -process material (CEMP- $s$  class; Beers & Christlieb 2005) from a companion star that passed through the AGB phase of evolution. The large oval identifies the location of the seven known highly  $r$ -process-enhanced stars in the Ret II UFD. The shaded box marks the location where this study seeks to identify field stars in the same region of the diagram occupied by the stars in UFD galaxies with low levels of  $n$ -capture elements. Upper limits have been omitted for clarity.

( $[\text{Fe}/\text{H}] \approx -3.0$ ) red giant that has been the subject of many studies since its discovery by Bond (1980). Three studies in the current century (Johnson & Bolte 2001; François et al. 2007; Roederer et al. 2014c) have reported detections of several  $n$ -capture elements in addition to Sr and Ba. These abundances are shown in Figure 2, where they have been normalized to the Eu abundance to account for small systematic shifts in the overall abundance scale. The  $\log(X/\text{Eu})$  ratios between a given element, X, and Eu agree among different studies within  $\sim 2\sigma$ . The level of  $n$ -capture abundances found in BD-18°5550 is among the lowest known:  $\log \epsilon(\text{Eu}) = -3.09 \pm 0.18$ ;  $[\text{Eu}/\text{H}] = -3.61 \pm 0.18$ ;  $[\text{Eu}/\text{Fe}] = -0.46 \pm 0.14$  (Roederer et al. 2014c).

CS 22185-007 is somewhat fainter ( $V \approx 13.4$ ) than BD-18°5550, but it is still considerably brighter than the brightest red giants in UFD galaxies. This metal-poor ( $[\text{Fe}/\text{H}] \approx -3.0$ ) giant was first identified by Beers et al. (1992), and Roederer et al. (2014c) performed the first abundance analysis on a high-resolution spectrum of this star. That study reported detections of one line of Nd II,

two lines of Eu II, and one line of Yb II. The abundances of  $n$ -capture elements in CS 22185-007 are also quite low:  $\log \epsilon(\text{Eu}) = -2.80 \pm 0.20$ ;  $[\text{Eu}/\text{H}] = -3.32 \pm 0.20$ ;  $[\text{Eu}/\text{Fe}] = -0.31 \pm 0.16$  (Roederer et al. 2014c).

CS 22891-200 is similarly faint ( $V \approx 13.9$ ). This metal poor ( $[\text{Fe}/\text{H}] \approx -3.9$ ) giant was first identified by Beers et al. (1985). McWilliam et al. (1995) performed the first detailed abundance analysis, and subsequent abundance work has been performed by McWilliam (1998), Andrievsky et al. (2011), Hollek et al. (2011), and Roederer et al. (2014c). The highest S/N spectrum of CS 22891-200 was examined by Roederer et al., who reported a detection of Eu from the two strongest Eu II lines in the blue. Eu is present in CS 22891-200 at an extremely low level:  $\log \epsilon(\text{Eu}) = -3.43 \pm 0.22$ ;  $[\text{Eu}/\text{H}] = -3.95 \pm 0.22$ ;  $[\text{Eu}/\text{Fe}] = -0.07 \pm 0.19$  (Roederer et al. 2014c).

Three lines are shown for comparison in the left panels of Figure 2. One is a theoretical prediction for the weak component of the  $s$ -process operating in a  $25 M_{\odot}$ , rapidly-rotating (at half the critical break-up velocity), low-metallicity ( $Z = 10^{-5}$ ,  $[\text{Fe}/\text{H}] \approx -3.2$ ) star (G. Ces-

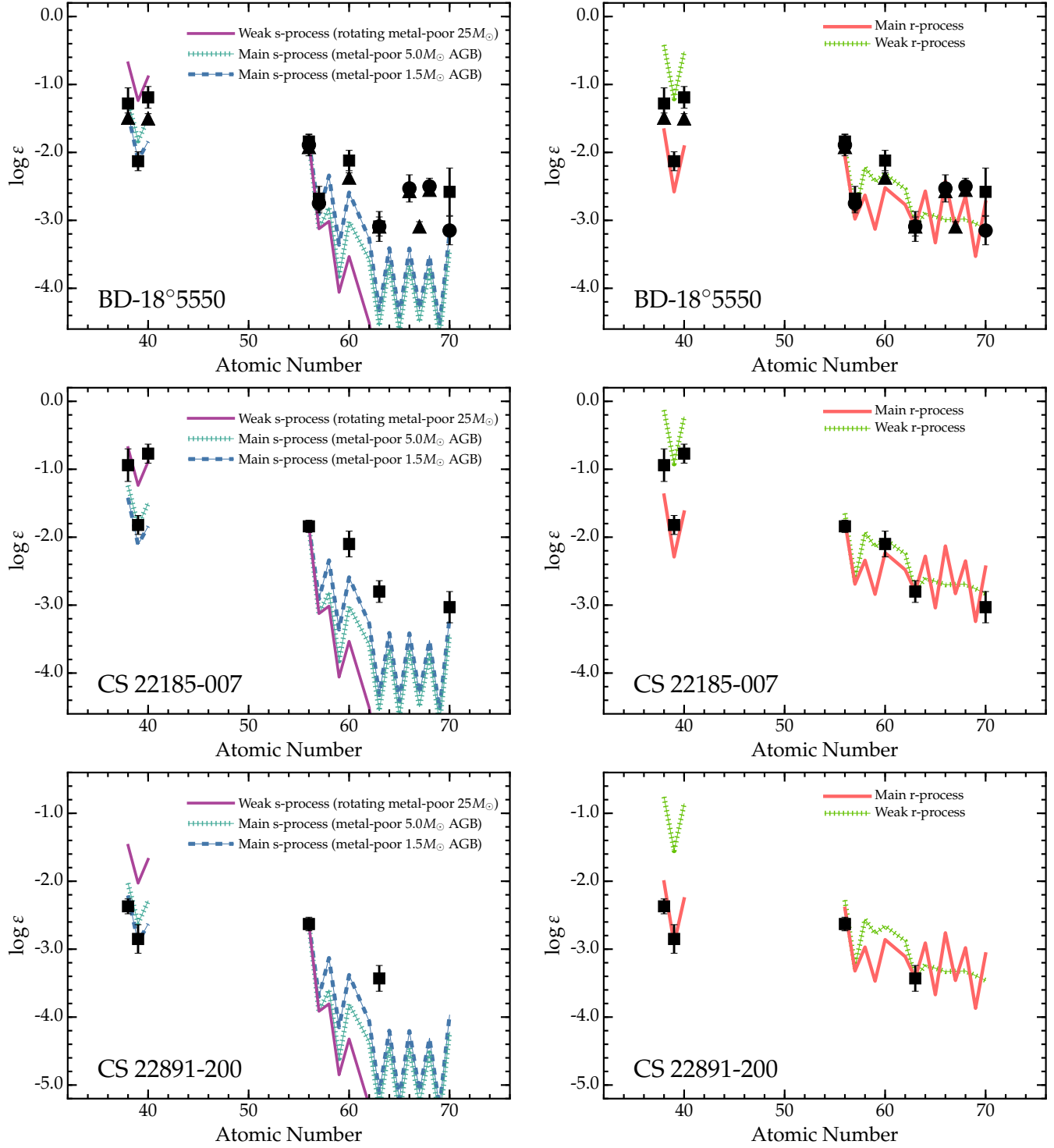


**Figure 2.** Log of the abundance as a function of atomic number. Three abundance studies are illustrated: the circles mark data from [Johnson & Bolte \(2001\)](#), the triangles mark data from [François et al. \(2007\)](#), and the squares mark data from [Roederer et al. \(2014c\)](#). The abundances for the three different studies of BD-18°5550 have been normalized to the Eu abundance from [Roederer et al.](#) In the left panels, the solid purple line indicates the template for the weak component of the  $s$ -process operating in massive, low-metallicity, rapidly-rotating stars ([Frischknecht et al. 2012, 2016](#)), the short-studded aqua line indicates the template for the main component of the  $s$ -process operating in a metal-poor  $5.0 M_{\odot}$  AGB star, and the long-studded blue line indicates the template for the main component of the  $s$ -process operating in a metal-poor  $1.5 M_{\odot}$  AGB star with the same parameters ([Cristallo et al. 2011, 2015](#)). These are normalized to the Ba abundance. In the right panels, the solid red line indicates the template for the main component of the  $r$ -process and the short-studded green line indicates the template for the weak component of the  $r$ -process. These are normalized to the Eu abundance. See Section 3 for details.

cutti 2016, private communication<sup>3</sup>; Frischknecht et al. 2012, 2016). The other two are theoretical predictions for the main component of the  $s$ -process operating in 5.0 and 1.5  $M_{\odot}$  AGB stars with  $Z = 10^{-4}$  ( $[\text{Fe}/\text{H}] \approx -2.2$ , the lowest metallicity available in the grid). These two are taken from the Full-Network Repository of Updated Isotopic Tables and Yields (FRUITY) database<sup>4</sup> (Cristallo et al. 2011, 2015). It is unlikely that star formation lasted long enough in UFD galaxies to incorporate yields from low- or intermediate-mass AGB stars, but these three predictions represent the range of  $s$ -process nucleosynthesis outcomes that could be expected from low-metallicity stars. It is immediately apparent from Figure 2 that all of the  $s$ -process templates are a poor representation of the Eu and heavier elements in the rare earth domain in these three stars. Changing the normalization point for the models does not affect this conclusion.

Two lines are shown for comparison in the right panels of Figure 2. One is a template for the main component of the  $r$ -process, which mirrors the solar system  $r$ -process residual pattern. This is formed by averaging the abundance patterns in the highly  $r$ -process-enhanced red giants CS 22892-052 and CS 31082-001 (Hill et al. 2002; Sneden et al. 2003a, 2009). Another is a template for the weak component of the  $r$ -process, which may result from an inefficient or incomplete  $r$ -process whose neutron flux is insufficient to flow to the heaviest  $n$ -capture elements (e.g., Truran et al. 2002). This template is formed by averaging together the abundance patterns in the red giants HD 88609 and HD 122563 (Honda et al. 2007). The templates for the main and weak components of the  $r$ -process are derived from other metal-poor red giant stars, so any effects due to, e.g., departures from local thermodynamic equilibrium should cancel when performing this relative comparison.

The two  $r$ -process templates provide much better representations of the observed abundance patterns, especially throughout the rare earth domain (Ba, La, Nd, Eu, Dy, Ho, Er, and Yb) in BD-18°5550 and CS 22185-007. There may be a preference in the BD-18°5550 data for the main component of the  $r$ -process; e.g., at Dy, Ho, and Er ( $Z = 66-68$ ). The CS 22185-007 data may favor the weak component of the  $r$ -process, especially at Yb ( $Z = 70$ ). The Sr, Y, and Zr ( $Z = 38-40$ ) abundances in BD-18°5550 and CS 22185-007 lie between the main and weak  $r$ -process patterns when normalized to Eu. The abundance pattern in CS 22891-200, though limited, favors the main component of the  $r$ -process. The elements in the rare earth domain in these stars are more than 2 orders of magnitude less abundant than in highly  $r$ -process-enhanced stars like CS 22892-052 or those in Ret II, yet they are still recognizable as having originated via some form of  $r$ -process nucleosynthesis.

The  $[\text{Eu}/\text{Ba}]$  ratio is a good quantitative discriminant of the nucleosynthetic origin of the elements in the rare earth domain. The  $[\text{Eu}/\text{Ba}]$  ratios in these three stars are supersolar:  $+0.41 \pm 0.16$ ,  $+0.69 \pm 0.17$ , and  $+0.86 \pm 0.20$  in BD-18°5550, CS 22185-007, and CS 22891-200, respectively. For comparison, Roederer et al. (2014a) found an average  $[\text{Eu}/\text{Ba}] = +0.71$  with a star-to-star disper-

sion of 0.19 dex for 13 highly  $r$ -process-enhanced stars drawn from the same survey and analyzed in an identical fashion. This is comparable to the  $[\text{Eu}/\text{Ba}]$  ratio expected from the solar  $r$ -process residuals,  $+0.92$  (e.g., Sneden et al. 2008; Bisterzo et al. 2011). The two stars frequently associated with the weak component of the  $r$ -process, HD 88609 and HD 122563, have  $[\text{Eu}/\text{Ba}] = +0.48 \pm 0.16$  and  $+0.53 \pm 0.18$  (Honda et al. 2007) or  $[\text{Eu}/\text{Ba}] = +0.33 \pm 0.16$  and  $+0.33 \pm 0.18$  (Roederer et al. 2014c). The solar (main)  $r$ -process and weak  $r$ -process values bracket the range of values found in the three stars of interest. In contrast, the  $[\text{Eu}/\text{Ba}]$  ratio expected from the  $s$ -process contribution to the solar system is  $-1.17$ . The ratios in these stars clearly prefer the  $r$ -process values.

None of the light element (C to Zn;  $6 \leq Z \leq 30$ ) abundances in BD-18°5550, CS 22185-007, or CS 22891-200 are unusual with respect to the metal-poor halo field population (Roederer et al. 2014b,c). BD-18°5550 and CS 22185-007 show enhancements in  $\alpha$  elements like Mg, Si, and Ca that are typical for metal-poor stars ( $[\alpha/\text{Fe}] \approx +0.4$ ; e.g., McWilliam et al. 1995; Cayrel et al. 2004). CS 22891-200 is enhanced in C ( $[\text{C}/\text{Fe}] \approx +1.0$  after correcting for evolutionary effects; Placco et al. 2014), N ( $[\text{N}/\text{Fe}] = +1.2$ ), and several  $\alpha$  elements (e.g.,  $[\text{Mg}/\text{Fe}] = +0.8$ ). These enhancements are common among stars in the class of carbon-enhanced metal-poor stars with no enhancement of neutron-capture elements (e.g., Ryan et al. 2005; Norris et al. 2013). Several stars have been found that show both carbon enhancement and  $r$ -process enhancement (e.g., Sneden et al. 2003a; Roederer et al. 2014c; Ji et al. 2016c). The iron-group elements in these stars show no deviations from the usual ratios, either. In summary, the light-element abundance patterns in these stars are typical among metal-poor stars in the halo and UFD galaxies.

#### 4. DISCUSSION AND CONCLUSIONS

Among 85 metal-poor halo field stars with detections of Sr and Ba in the shaded region of Figure 1, only 3 of them have compelling detections of additional elements heavier than Ba. There is no known association between these field stars and disrupted satellite galaxies. These stars could have formed in UFD galaxies that were later disrupted, but the result of this study does not rely on such speculation. These stars provide the first definitive evidence that  $r$ -process nucleosynthesis can produce ratios consistent with the  $[\text{Sr}/\text{Ba}]$  and  $[\text{Ba}/\text{Fe}]$  ratios found in most UFD galaxies.

As can be seen in Figure 1, and which was found previously by Frebel et al. (2016) and Ji et al. (2016c), the  $[\text{Sr}/\text{Ba}]$  ratios in most UFD galaxies span a range of several dex. This range overlaps with the  $[\text{Sr}/\text{Ba}]$  ratios found in the highly  $r$ -process-enhanced stars in Ret II, hinting that the heavy elements in the other UFD galaxies could reflect the same  $r$ -process pattern diluted into a larger mass of Fe. Two of the three field stars examined here, BD-18°5550 and CS 22891-200, also fall into this range. A substantial fraction of stars in the UFD galaxies and the field star CS 22185-007 have solar or super-solar  $[\text{Sr}/\text{Ba}]$  ratios that are inconsistent with the  $r$ -process enhanced stars in Ret II. This indicates that an additional nucleosynthesis mechanism may be responsible. This additional process could correspond to the

<sup>3</sup> <http://www.astro.keele.ac.uk/shyne/datasets/s-process-yields-from-frischknecht-et-al-12-15>

<sup>4</sup> <http://fruity.oa-teramo.inaf.it/modelli.pl>

weak  $r$ -process (e.g., Wanajo 2013), truncated  $r$ -process (Boyd et al. 2012; Aoki et al. 2013b), or weak  $s$ -process (e.g., Frischknecht et al. 2016). If a weak or truncated  $r$ -process is responsible, it would need to be capable of producing variable [Sr/Ba] yields and relatively normal  $r$ -process ratios within the rare earth domain. If a weak  $s$ -process is responsible, it would need to be capable of producing variable [Sr/Ba] yields, and its products would need to be mixed with a small amount of  $r$ -process material before being incorporated into the stars observed today.

Cescutti et al. (2013) were able to reproduce the spread in [Sr/Ba] ratios in metal-poor halo stars using a combination of a main  $r$ -process component from supernovae and a weak  $s$ -process component from massive, rapidly-rotating, low-metallicity stars. Their model predicts that the stars with high [Sr/Ba] ratios should show  $s$ -process signatures. Cescutti & Chiappini (2014) and Cescutti et al. (2015) considered other sites for the  $r$ -process nucleosynthesis, including the mergers of binary neutron star systems and magneto-rotational supernovae. These models predict that the stars with low [Sr/Ba] ratios should show  $r$ -process signatures, in agreement with observations. These models also predict that metal-poor stars with high [Sr/Ba] ratios should show  $s$ -process signatures, independent of the site of the  $r$ -process. The results of the present study suggest an observational test of these models: derivation of the abundance pattern within the rare earth domain in stars with [Sr/Ba] > 0 and [Ba/Fe] < -1.0 or so. The Cescutti et al. (2015) models may be capturing several important pieces of physics, like the mass range of stars where the  $n$ -capture nucleosynthesis operates or the typical mass of H or Fe into which the  $n$ -capture elements are diluted, for example. Future theoretical work should address whether these scenarios can also be applied to environments that give rise to today's population of UFD galaxies (cf. Tsujimoto & Shigejima 2014; Ishimaru et al. 2015). Future theoretical work should also address whether the massive, rapidly-rotating, low-metallicity stars that are proposed to produce a weak  $s$ -process might also produce a small amount of  $r$ -process material during the subsequent supernova explosion.

Certainly the most direct observational approach to test these assertions is to detect additional  $n$ -capture elements in stars in the UFD galaxies themselves. This may require the use of high-resolution echelle spectrographs on 20–30 m class telescopes, like the G-CLEF instrument (Szentgyorgyi et al. 2014) being developed for the Giant Magellan Telescope. In the meantime, the results presented here may offer the next-best observational guidance for interpreting the heavy element abundance patterns in most UFD galaxies.

I thank G. Cescutti, J. Cowan, and A. Ji for supportive comments on an early version of this manuscript, and I thank G. Cescutti for sending model predictions in tabular form. I also thank the referees, G. Preston and an anonymous referee, for their helpful recommendations. I acknowledge partial support from grant PHY 14-30152 (Physics Frontier Center/JINA-CEE) awarded by the U.S. National Science Foundation. This research has made use of NASA's Astrophysics Data System Biblio-

graphic Services; the arXiv pre-print server operated by Cornell University; the SIMBAD and VizieR database hosted by the Strasbourg Astronomical Data Center; and the matplotlib (Hunter 2007), numpy (van der Walt et al. 2011), and scipy (Jones et al. 2001) Python libraries.

## REFERENCES

- Andrievsky, S. M., Spite, F., Korotin, S. A., et al. 2011, *A&A*, 530, A105
- Aoki, W., Beers, T. C., Honda, S., & Carollo, D. 2010, *ApJ*, 723, L201
- Aoki, W., Beers, T. C., Lee, Y. S., et al. 2013a, *AJ*, 145, 13
- Aoki, W., Frebel, A., Christlieb, N., et al. 2006, *ApJ*, 639, 897
- Aoki, W., Honda, S., Beers, T. C., et al. 2005, *ApJ*, 632, 611
- Aoki, W., Norris, J. E., Ryan, S. G., Beers, T. C., & Ando, H. 2002, *ApJ*, 567, 1166
- Aoki, W., Norris, J. E., Ryan, S. G., et al. 2004, *ApJ*, 608, 971
- Aoki, W., Suda, T., Boyd, R. N., Kajino, T., & Famiano, M. A. 2013b, *ApJ*, 766, L13
- Barklem, P. S., Christlieb, N., Beers, T. C., et al. 2005, *A&A*, 439, 129
- Bechtol, K., Drlica-Wagner, A., Balbinot, E., et al. 2015, *ApJ*, 807, 50
- Beers, T. C., & Christlieb, N. 2005, *ARA&A*, 43, 531
- Beers, T. C., Preston, G. W., & Shectman, S. A. 1985, *AJ*, 90, 2089
- Beers, T. C., Preston, G. W., & Shectman, S. A. 1992, *AJ*, 103, 1987
- Bisterzo, S., Gallino, R., Straniero, O., Cristallo, S., Käppeler, F. 2011, *MNRAS*, 418, 284
- Bond, H. E. 1980, *ApJS*, 44, 517
- Bonifacio, P., Spite, M., Cayrel, R., et al. 2009, *A&A*, 501, 519
- Boyd, R. N., Famiano, M. A., Meyer, B. S., et al. 2012, *ApJ*, 744, L14
- Brown, T. M., Tumlinson, J., Geha, M., et al. 2014, *ApJ*, 796, 91
- Burris, D. L., Pilachowski, C. A., Armandroff, T. E., et al. 2000, *ApJ*, 544, 302
- Carretta, E., Gratton, R., Cohen, J. G., Beers, T. C., & Christlieb, N. 2002, *AJ*, 124, 481
- Cayrel, R., Depagne, E., Spite, M., et al. 2004, *A&A*, 416, 1117
- Cescutti, G., & Chiappini, C. 2014, *A&A*, 565, A51
- Cescutti, G., Chiappini, C., Hirschi, R., Meynet, G., & Frischknecht, U. 2013, *A&A*, 553, A51
- Cescutti, G., Romano, D., Matteucci, F., Chiappini, C., & Hirschi, R. 2015, *A&A*, 577, A139
- Cohen, J. G., Christlieb, N., McWilliam, A., et al. 2008, *ApJ*, 672, 320-341
- Cohen, J. G., Christlieb, N., Thompson, I., et al. 2013, *ApJ*, 778, 56
- Cristallo, S., Piersanti, L., Straniero, O., et al. 2011, *ApJS*, 197, 17
- Cristallo, S., Straniero, O., Piersanti, L., & Gobrecht, D. 2015, *ApJS*, 219, 40
- Depagne, E., Hill, V., Christlieb, N., & Primas, F. 2000, *A&A*, 364, L6
- François, P., Depagne, E., Hill, V., et al. 2007, *A&A*, 476, 935
- François, P., Monaco, L., Bonifacio, P., et al. 2016, *A&A*, 588, A7
- Frebel, A., & Norris, J. E. 2015, *ARA&A*, 53, 631
- Frebel, A., Norris, J. E., Gilmore, G., & Wyse, R. F. G. 2016, *ApJ*, 826, 110
- Frebel, A., Simon, J. D., Geha, M., & Willman, B. 2010, *ApJ*, 708, 560
- Frebel, A., Simon, J. D., & Kirby, E. N. 2014, *ApJ*, 786, 74
- Frischknecht, U., Hirschi, R., Pignatari, M., et al. 2016, *MNRAS*, 456, 1803
- Frischknecht, U., Hirschi, R., & Thielemann, F.-K. 2012, *A&A*, 538, L2
- Gratton, R. G., & Sneden, C. 1994, *A&A*, 287, 927
- Hansen, C. J., Nordström, B., Bonifacio, P., et al. 2011, *A&A*, 527, A65
- Hansen, T., Hansen, C. J., Christlieb, N., et al. 2015, *ApJ*, 807, 173
- Hill, V., Plez, B., Cayrel, R., et al. 2002, *A&A*, 387, 560
- Hunter, J.D. 2011, *Computing in Science & Engineering*, 9, 90

- Hollek, J. K., Frebel, A., Roederer, I. U., et al. 2011, *ApJ*, 742, 54
- Honda, S., Aoki, W., Beers, T. C., & Takada-Hidai, M. 2011, *ApJ*, 730, 77
- Honda, S., Aoki, W., Ishimaru, Y., & Wanaajo, S. 2007, *ApJ*, 666, 1189
- Honda, S., Aoki, W., Kajino, T., et al. 2004, *ApJ*, 607, 474
- Ishigaki, M. N., Aoki, W., Arimoto, N., & Okamoto, S. 2014, *A&A*, 562, A146
- Ishimaru, Y., Wanaajo, S., & Prantzos, N. 2015, *ApJ*, 804, L35
- Ivans, I. I., Sneden, C., James, C. R., et al. 2003, *ApJ*, 592, 906
- Jacobson, H. R., Keller, S., Frebel, A., et al. 2015, *ApJ*, 807, 171
- Ji, A. P., Frebel, A., Chiti, A., & Simon, J. D. 2016a, *Nature*, 531, 610
- Ji, A. P., Frebel, A., Ezzeddine, R., & Casey, A. R. 2016b, *ApJ*, submitted (arXiv:1609.02915)
- Ji, A. P., Frebel, A., Simon, J. D., & Chiti, A. 2016c, *ApJ*, 830, 93
- Ji, A. P., Frebel, A., Simon, J. D., & Geha, M. 2016d, *ApJ*, 817, 41
- Johnson, J. A. 2002, *ApJS*, 139, 219
- Johnson, J. A., & Bolte, M. 2001, *ApJ*, 554, 888
- Jones, E., Oliphant, E., Peterson, P., et al. 2001, *SciPy: Open Source Scientific Tools for Python*, <http://www.scipy.org>
- Koch, A., & Rich, R. M. 2014, *ApJ*, 794, 89
- Koch, A., Feltzing, S., Adén, D., & Matteucci, F. 2013, *A&A*, 554, A5
- Lai, D. K., Bolte, M., Johnson, J. A., et al. 2008, *ApJ*, 681, 1524
- Lai, D. K., Johnson, J. A., Bolte, M., & Lucatello, S. 2007, *ApJ*, 667, 1185
- Lee, D. M., Johnston, K. V., Tumlinson, J., Sen, B., & Simon, J. D. 2013, *ApJ*, 774, 103
- Mashonkina, L., Christlieb, N., Barklem, P. S., et al. 2010, *A&A*, 516, A46
- Mashonkina, L., Christlieb, N., & Eriksson, K. 2014, *A&A*, 569, A43
- McConnachie, A. W. 2012, *AJ*, 144, 4
- McWilliam, A. 1998, *AJ*, 115, 1640
- McWilliam, A., Preston, G. W., Sneden, C., & Searle, L. 1995, *AJ*, 109, 2757
- Mishenina, T. V., & Kovtyukh, V. V. 2001, *A&A*, 370, 951
- Norris, J. E., Yong, D., Bessell, M. S., et al. 2013, *ApJ*, 762, 28
- Norris, J. E., Yong, D., Gilmore, G., & Wyse, R. F. G. 2010, *ApJ*, 711, 350
- Placco, V. M., Beers, T. C., Reggiani, H., & Meléndez, J. 2016, *ApJ*, 829, L24
- Placco, V. M., Frebel, A., Beers, T. C., & Stancliffe, R. J. 2014, *ApJ*, 797, 21
- Placco, V. M., Frebel, A., Lee, Y. S., et al. 2015, *ApJ*, 809, 136
- Preston, G. W., & Sneden, C. 2000, *AJ*, 120, 1014
- Preston, G. W., & Sneden, C. 2001, *AJ*, 122, 1545
- Preston, G. W., Sneden, C., Thompson, I. B., Sheckman, S. A., & Burley, G. S. 2006, *AJ*, 132, 85
- Roederer, I. U. 2013, *AJ*, 145, 26
- Roederer, I. U., & Kirby, E. N. 2014, *MNRAS*, 440, 2665
- Roederer, I. U., & Lawler, J. E. 2012, *ApJ*, 750, 76
- Roederer, I. U., Cowan, J. J., Preston, G. W., et al. 2014a, *MNRAS*, 445, 2970
- Roederer, I. U., Karakas, A. I., Pignatari, M., & Herwig, F. 2016a, *ApJ*, 821, 37
- Roederer, I. U., Mateo, M., Bailey, J. I., III, et al. 2016b, *AJ*, 151, 82
- Roederer, I. U., Preston, G. W., Thompson, I. B., Sheckman, S. A., & Sneden, C. 2014b, *ApJ*, 784, 158
- Roederer, I. U., Preston, G. W., Thompson, I. B., et al. 2014c, *AJ*, 147, 136
- Roederer, I. U., Sneden, C., Thompson, I. B., Preston, G. W., & Sheckman, S. A. 2010, *ApJ*, 711, 573
- Ryan, S. G., Aoki, W., Norris, J. E., & Beers, T. C. 2005, *ApJ*, 635, 349
- Ryan, S. G., Norris, J. E., & Beers, T. C. 1996, *ApJ*, 471, 254
- Ryan, S. G., Norris, J. E., & Bessell, M. S. 1991, *AJ*, 102, 303
- Simon, J. D., Frebel, A., McWilliam, A., Kirby, E. N., & Thompson, I. B. 2010, *ApJ*, 716, 446
- Sivarani, T., Beers, T. C., Bonifacio, P., et al. 2006, *A&A*, 459, 125
- Sneden, C., Cowan, J. J., & Gallino, R. 2008, *ARA&A*, 46, 241
- Sneden, C., Cowan, J. J., Lawler, J. E., et al. 2003a, *ApJ*, 591, 936
- Sneden, C., Lawler, J. E., Cowan, J. J., Ivans, I. I., & Den Hartog, E. A. 2009, *ApJS*, 182, 80
- Sneden, C., Preston, G. W., & Cowan, J. J. 2003b, *ApJ*, 592, 504
- Szentgyorgyi, A., Barnes, S., Bean, J., et al. 2014, *Proc. SPIE*, 9147, 914726
- Tsujimoto, T., & Shigeyama, T. 2014, *A&A*, 565, L5
- Truran, J. W., Cowan, J. J., Pilachowski, C. A., & Sneden, C. 2002, *PASP*, 114, 1293
- van der Walt, S., Colbert, S. C., Varoquaux, G. 2011, *Computing in Science & Engineering*, 13, 22
- Wanaajo, S. 2013, *ApJ*, 770, L22
- Yong, D., Norris, J. E., Bessell, M. S., et al. 2013, *ApJ*, 762, 26